infants simply do not perceive the difference between the two stimuli because of limitations in their eye and early visual processing. We can exclude this explanation because analysis of the low-frequency transient visual ERPs elicited by the Kanizsa square and the control stimuli showed significant effects of stimulus for both the 6- and the 8-month-old groups (Fig. 3A). Second, it may be that gammalike effects can be observed at lower frequencies in 6-month-old infants than in adults and 8-month-olds. To examine this possibility, we analyzed oscillatory activity at a lower frequency range (21 to 32 Hz) but still failed to find equivalent binding-related bursts corresponding to those reported in the gamma-band frequency in older participants.

22. The between-subject SD of the latency of peak gamma activity after Kanizsa square stimulus at the three left frontal electrodes (Fig. 2) was 76.4 ms and 113.3 ms in 8- and 6-month-olds, respectively. The SD of the latency of minimal gamma activity after the control stimulus was 57.7 ms and 93.1 ms in 8- and 6-month-olds, respectively.
23. M. Sugawara, T. Morotomi, *Scand. J. Psychol.* **32**, 352 (1991).
24. Both adults (*3*, *11*, *23*) and 8-month-olds show a more negative ERP over the occipital cortex in response to Kanizsa figures than to control stimuli from about 120 ms after stimulus presentation.
25. D. H. Ffytche, S. Zeki, *Neuroimage* **3**, 104 (1996).
26. C. Tallon-Baudry, O. Bertrand, C. Wienbruch, B. Ross, C. Pantev, *Neuroreport* **8**, 1103 (1997).
27. G. Csibra, L. A. Tucker, M. H. Johnson, *Int. J. Psychophysiol.* **29**, 210 (1998).
28. We selected four regions for statistical comparisons on the basis of previous works: bilateral occipital areas (*25*) and bilateral frontal areas (*11*). Only the statistically reliable effects are reported.
29. The ERPs were digitally filtered with an elliptical low-pass filter at 35 Hz and converted to an average reference.

30. We thank L. Tucker and Á. Volein for their assistance in recording and coding data, and the UK Medical Research Council (program grant G9715587), the European Commission (BioMed grant BMH4-CT97-2032), the Royal Society, and Birkbeck College for support of this project.

20 June 2000; accepted 23 October 2000

"Fluorescent Timer": Protein That Changes Color with Time

Alexey Terskikh,[1]* Arkady Fradkov,[2] Galina Ermakova,[2] Andrey Zaraisky,[2] Patrick Tan,[1] Andrey V. Kajava,[3] Xiaoning Zhao,[4] Sergey Lukyanov,[2] Mikhail Matz,[2] Stuart Kim,[1] Irving Weissman,[1] Paul Siebert[4]

We generated a mutant of the red fluorescent protein drFP583. The mutant (E5) changes its fluorescence from green to red over time. The rate of color conversion is independent of protein concentration and therefore can be used to trace time-dependent expression. We used in vivo labeling with E5 to measure expression from the heat shock–dependent promoter in *Caenorhabditis elegans* and from the *Otx-2* promoter in developing *Xenopus* embryos. Thus, E5 is a "fluorescent timer" that can be used to monitor both activation and down-regulation of target promoters on the whole-organism scale.

Green fluorescent protein (GFP) from the luminescent jellyfish *Aequorea victoria* is an important tool in molecular and cellular biology as a transcriptional reporter, fusion tag, or biosensor (*1*). The recent discovery of GFP-like fluorescent proteins from nonbioluminescent *Anthozoa* species (*2*), in particular the red fluorescent protein drFP583, has opened new horizons for multicolor labeling and fluorescence resonance energy transfer applications.

An earlier report (*2*) suggested that the red fluorophore of drFP583 requires an additional autocatalytic modification of a GFP-like fluorophore. We thus generated mutants of drFP583 using error-prone polymerase chain reaction (PCR) (*3*) and screened for mutants exhibiting a green intermediate fluorescence (*4*).

Mutations resulted in proteins with varying fluorescent properties, such as faster maturation, double emission (green and red), or exclusive green fluorescence. Of particular interest was the E5 mutant, which changes its fluorescence over time. This mutant changed from initial bright green fluorescence to yellow, orange, and finally red over time (Fig. 1, A and B). Yellow and orange fluorescence indicate that the protein species with green and red fluorophores are both present (Fig. 1B, color insert). The existence of a green-emitting intermediate suggests that E5 maturation involves the modification of a GFP-like fluorophore to give the red fluorophore. Changing the temperature had the same effect on the rates of decay of green fluorescence and growth of red fluorescence, which suggests that these processes reflect the same chemical reaction (Fig. 1B). In addition, the overall reaction speed was independent of the initial concentration of E5 protein in the range from 10 μg/ml to 1 mg/ml (as in Fig. 1B). It was also insensitive to variations in ionic strength in the range from 10 mM to 1 M NaCl, to the presence of 150 mM EDTA, or to changes in pH between 7.0 and 8.0. pH values below 4.5 or above 12 resulted in the disappearance of the red-shifted absorption and the appearance of 386-nm or 448-nm absorption peaks for acid and alkali, respectively (this was also observed for drFP583) (Fig. 1D). This is strikingly similar to the absorption spectra of GFP— 383 nm and 446 nm for acid and alkali, respectively (*5*)—in which the pH-dependent shift between 383 and 446 nm is due to ionization of the fluorophore phenolic group (*6*). The maturation from green to red fluorescence slows down considerably in deoxygenated buffer, suggesting that the fluorophore modification requires molecular oxygen. The properties of E5 provide insight into the nature of the red fluorophore; for instance, we detected similar fluorescence dynamics in drFP583, although barely detectable changes in green fluorescence make it unsuitable for practical application (Fig. 1C).

As compared to drFP583, E5 has two substitutions: $Val^{105} \rightarrow Ala^{105}$ (V105A) and $Ser^{197} \rightarrow Thr^{197}$ (S197T). The impact of each substitution on the fluorescent properties of E5 was assessed in single mutants. Mutation V105A resulted in a twofold increase in fluorescence quantum yield as compared to drFP583 but no spectral shifts, whereas the S197T mutant essentially recapitulated the fluorescent timer phenotype. We modeled the structure of drFP583 on the basis of GFP crystal structure (*7*) (details of modeling are available at www.sciencemag.org/cgi/content/full/290/5496/1585/DC1 and the atomic coordinates are available at http://cmm.info.nih.gov/kajava) and found that Ser^{197} in drFP583 is analogous to Thr^{203} in GFP. Thr^{203} is in direct contact with the fluorophore (*7*, *8*), and replacements at this position invariably alter the fluorescent properties of GFP (*9*–*12*).

E5 has the potential to function as a fluorescent clock, giving temporal and spatial information on target promoter activity. Green fluorescent areas would indicate recent activation, yellow-to-orange regions would signify continuous promoter activity, and red fluorescent cells and tissues would denote areas in which promoter activity has ceased after an extended "on" period. In vitro, the rate of color conversion (the red:green ratio) is independent of the protein concentration, suggesting that it will not depend on the expression level within a cell. Given the superior in vivo stability of drFP583 as compared to GFP (*2*), protein degradation of either the green or red form is unlikely to be a problem. This approach would make it possible to discriminate changes in gene expres-

[1]School of Medicine, Stanford University, Stanford, CA 94305, USA. [2]Institute of Bioorganic Chemistry, Russian Academy of Science, 117871 Moscow, Russia. [3]Center for Molecular Modeling, Center for Information Technology, NIH, Building 12A, Bethesda, MD 20892, USA. [4]Clontech Laboratories, 1020 East Meadow Circle, Palo Alto, CA 94303, USA.

*To whom correspondence should be addressed. E-mail: Alexey.Terskikh@Stanford.edu

sion from the effects of morphogenetic displacement of expressing and nonexpressing cells. None of the existing techniques (such as in situ hybridization, immunostaining, or tracing of any known reporter) can achieve that. We analyzed the expression of E5 in three heterologous systems: mammalian cells, *C.* elegans, and *Xenopus*.

We characterized E5 in a HEK 293 mammalian cell line engineered with Tet-On or Tet-Off expression systems (*13*). For 293 Tet-On cells transfected with E5, a distinct green fluorescence was visible and was detected by flow cytometry between 6 and 9 hours after induction, whereas cells with both green and red fluorescence appeared after 9 hours after induction (Fig. 2A). Similar to bacterial expression, in mammalian cells, red fluorescence developed faster in the E5 mutant than in wild-type drFP583 protein (Fig. 2A). When 293 Tet-Off cells were used, the majority of cells initially demonstrated strong green and red fluorescence at the beginning (a fully induced promoter) but lost the strong green fluorescence upon transcription shutdown. These changes could be readily observed under a fluorescence microscope (Fig. 2B). The persistence of strong green fluorescence in some cells was due to the inevitable heterogeneity of transient transfection, including the abnormal accumulation of mRNA in some cells and promoter leakiness.

To demonstrate the utility of the fluorescent timer as a tool for studying promoter activity in specific organisms, the E5 mutant was placed under the control of the *C. elegans* heat shock promoter *hsp 16-41*. This promoter exhibits minimal expression in unstressed animals, robust induction of transcription after heat shock, and rapid inactivation upon subsequent recovery to ambient temperature (*14*). An *hsp-E5* transgene was microinjected into worms, and several independent lines carrying the transgene as an extrachromosomal array were established (*15*). No fluorescence was observed in [*hsp-E5*(+)] worms maintained at ambient temperatures (*16*). However, after a standard heat shock regime (1 hour at 33°C), green fluorescence was observed in embryos as early as 2 hours into the recovery period (Fig. 3). Red fluorescence was detected in [*hsp-E5*(+)] embryos at 5 hours after heat shock (Fig. 3) and increased in intensity over time, so that at 50 hours after heat shock, the red:green signal ratio was close to 9:1. Similar kinetics of the fluorescent timer were observed in [*hsp-E5*(+)] worms at larval and adult stages. The prolonged periods of green fluorescence observed in these experiments are due to stabilization of the E5 mRNA, caused by the presence of a 3′ untranslated region (UTR) derived from the *unc-54* gene (*17*). In our experiments, the color hue of transgenic embryos at different time points after heat shock could be readily distinguished by eye (Fig. 3A, overlay). Moreover, within experimental error, the red:green fluorescence ratio changed linearly with time (at least within the first 14 hours), thus providing a unique measurement of time elapsed since the heat shock. Remarkably, despite considerable heterogeneity in the absolute fluorescence intensities of individual embryos at any

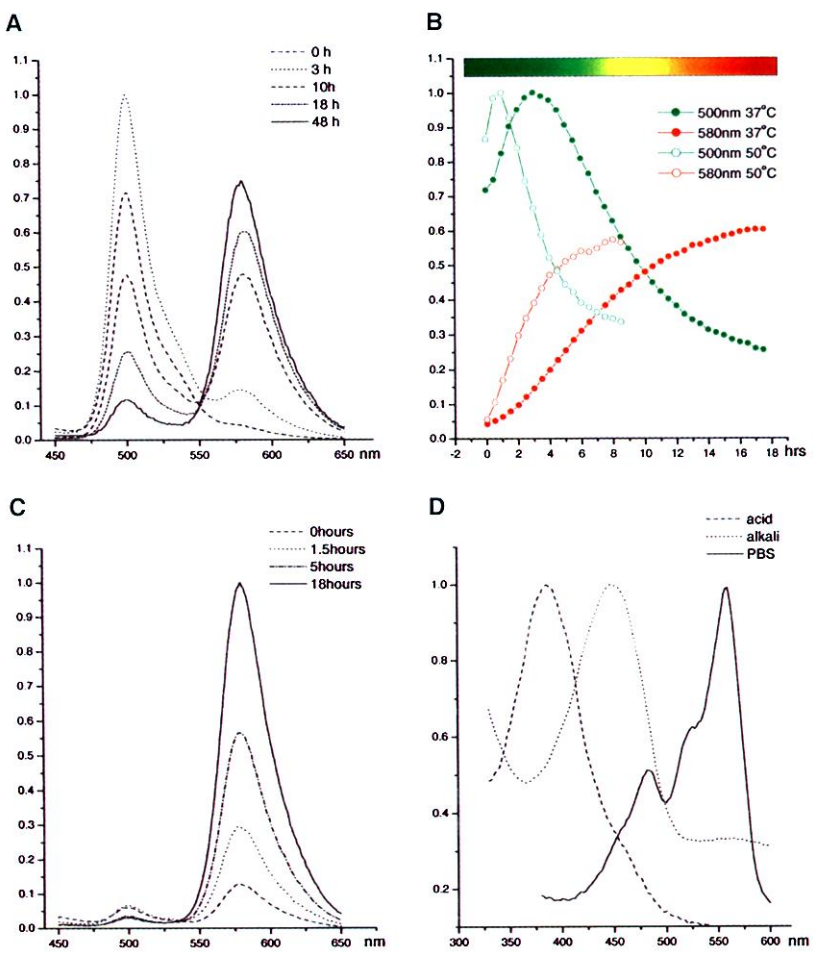

Fig. 1. In vitro analysis of the E5 mutant. All spectra are normalized; 0 hours refers to the first measurement performed on the freshly purified protein. (**A** and **C**) Emission spectra of E5 (A) and drFP583 (C), excited at 280 nm during the course of fluorescence development. (**B**) Time course of green (500 nm) and red (580 nm) fluorescence development in E5 at 37° and 50°C; the color bar represents the overlay color of green and red fluorescence at each time point at 37°C. (**D**) Absorption spectra of acid- (NaOAc, pH 4.5) or alkali- (NaOH, pH 12) denatured E5; PBS denotes E5 absorption in PBS.

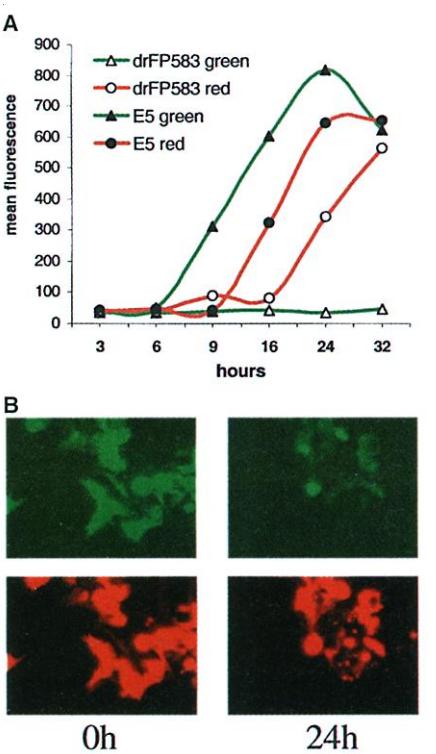

Fig. 2. Transient expression of drFP583 and the E5 mutant in Tet-On/Off systems. (**A**) FACS analysis of 293 Tet-On cells. Transcription was induced at 0 hours. Triangles, fluorescence in the FL1 (FITC) channel; circles, fluorescence in the FL2 (PE) channel. (**B**) Fluorescence images of 293 Tet-Off cells transfected with the E5 mutant; transcription was shut down at 0 hours.

given time point, the red:green fluorescence ratios among embryos at the same time point were similar, as is expected for an autocatalytic reaction causing the color transition. In addition, the fluorescent ratio was uniform throughout the embryo (Fig. 3, overlay), despite differences in monitored cell types; indicating that, at least under our experimental conditions, the process of E5 maturation is independent of the cellular environment.

We also used the E5 mutant to trace the activity of the *Otx-2* promoter. The homeobox gene *Otx-2* is involved in the patterning of anterior structures, which are common to all bilaterian animals (*18*). In *Xenopus*, at the midgastrula stage, the major domain of *Otx-2* expression is in the head neuroectoderm. As development proceeds, the expression is almost completely suppressed in parts of this domain, namely, in the presumptive rostral area, telencephalon, and ventral diencephalon (*19*). Thus, in the tadpole's brain, *Otx-2* expression revealed by in situ hybridization is strong in the mesencephalon and dorsal diencephalon but is much weaker in the telencephalon and ventral diencephalon (Fig. 4C). We assembled a plasmid containing the E5 gene under the control of the *Xenopus Otx-2* promoter and microinjected this into both dorsal blastomers of the *X. laevis* embryo at the eight-cell stage (*20*). The representative mosaic fluorescent image composed from clones of cells, which acquired the plasmid during blastomere cleavage (*21*), reflects the in situ hybridization data accurately (Fig. 4, A to C). The telencephalon and rostral region of the tadpole are marked orange, indicating that the *Otx-2* promoter was once active there but is now mostly silent, giving the accumulated protein time to mature. Simultaneously, the mesencephalon and ventral diencephalon are green, indicating that *Otx-2* promoter activity is driving expression of E5 in these regions. In a control experiment, the expression of E5 was driven by the promoter of another homeobox gene, *Xanf-1*. The expression of *Xanf-1* also occurs in neuroectoderm, but, unlike *Otx-2*, does not have distinct spatiotemporal domains and ceases before the tadpole stage (*21*, *22*). Correspondingly, the signal from the *Xanf-1*/E5 construct appeared uniformly orange in the tadpole brain (Fig. 4D).

"Fluorescent timer" provides an easy and reliable way to analyze the "history" of gene expression and gives the ability to monitor two equally important processes: activation and down-regulation of gene expression. The ability to evaluate promoter activity over a wide time range by analyzing a single developmental stage raises the possibility of large-scale screening for new time-dependent promoters, many of which are associated with development control genes.

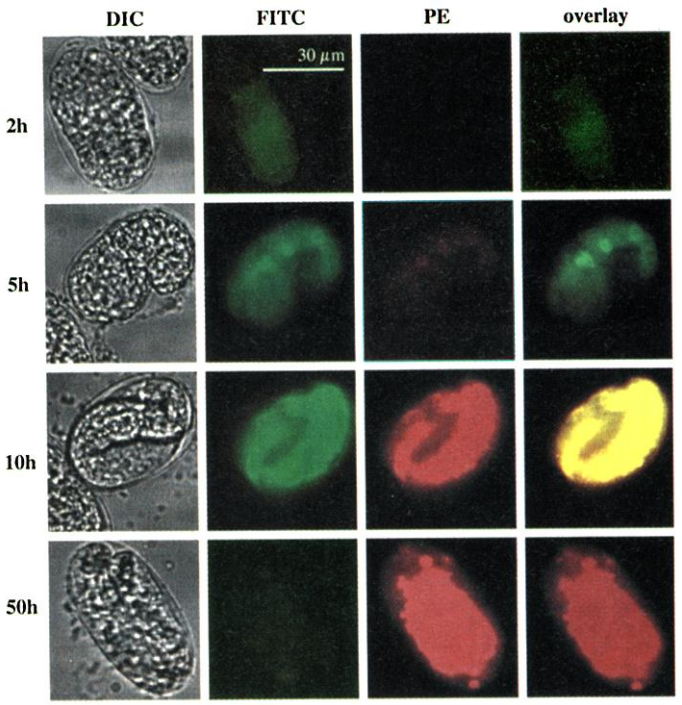

Fig. 3. Heat shock–regulated expression of the E5 mutant in *C. elegans*. Representative images of [*hsp-E5*(+)] embryos are shown: the bright field (DIC), FITC filter, PE filter, and the overlay, after 2, 5, 10, and 50 hours after the heat shock.

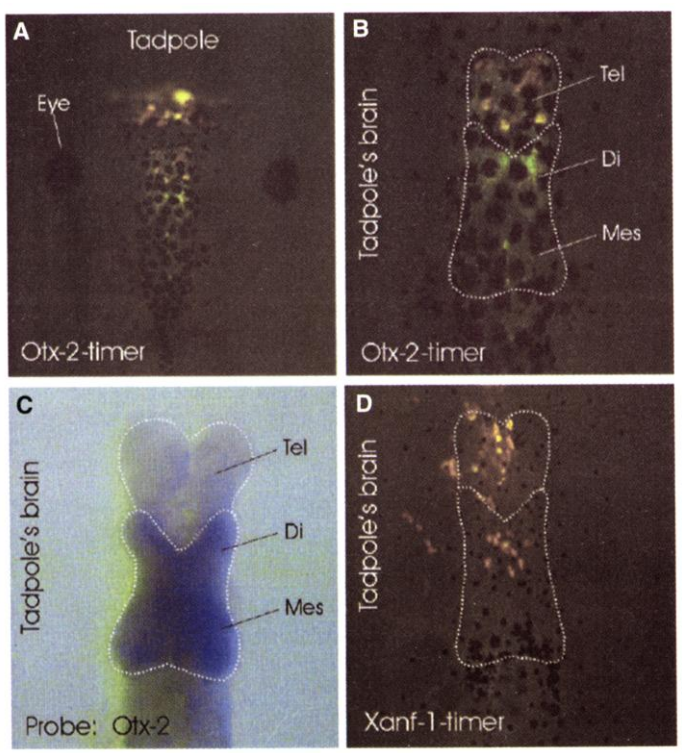

Fig. 4. Expression of E5 (timer) in a developing *Xenopus* embryo; fully matured E5 appears orange because of the FITC filter set. (**A**) Dorsal view of the tadpole expressing E5 under the control of the *Otx-2* promoter; only some cells express the E5 protein because of the mosaic distribution of plasmids within the embryo. (**B**) Brain region of the tadpole shown in (A). Telencephalic (Tel) and di- and mesencephalic (Di and Mes) borders are designated by a dotted line (**C**) Dorsal view of the whole-mount in situ hybridization of the tadpole brain with an *Otx-2* probe. (**D**) Dorsal view of the brain region of the tadpole expressing E5 under the control of the *Xanf-1* promoter.

References and Notes

1. R. Y. Tsien, *Annu. Rev. Biochem.* **67**, 509 (1998).
2. M. V. Matz *et al.*, *Nature Biotechnol.* **17**, 969 (1999).
3. R. C. Cadwell, G. F. Joyce, *PCR Methods Appl.* **2**, 28 (1992).
4. Random mutagenesis was performed with Diversity PCR Random Mutagenesis kit (Clontech) according to the manufacturer's protocol optimized for three to four mutations per 1000 base pairs. PCR products were cloned into pQE-30/Bam HI/Hind III vector. *Escherichia coli* DH5-α (Clontech) were transformed by electroporation in 10% glycerol with ligation mixture and were grown on Luria broth (LB)/agar/Amp plates with 0.1 mM isopropyl-β-D-thiogalactopyranoside at 37°C overnight. Colonies (up to 2000 to 5000 per plate) were screened visually, using a fluorescent microscope (Karl Zeiss) with 31001 filter set (Chroma). For study of fluorescence kinetics, bacteria harboring the recombinant plasmid were grown overnight on the LB plates at high density, scraped, resuspended in ice-cold phosphate-buffered saline (PBS), and sonicated. The lysate was cleared by centrifugation at 4°C, and the protein was purified from

the supernatant on ice with TALON resin (Clontech). All spectra were measured on purified proteins with a LS50B Luminescence Spectrometer (Perkin-Elmer).
5. R. Y. Tsien, *Annu. Rev. Biochem.* **67**, 509 (1998).
6. H. Niwa *et al.*, *Proc. Natl. Acad. Sci. U.S.A* **93**, 13617 (1996).
7. M. Ormo *et al.*, *Science* **273**, 1392 (1996).
8. F. Yang, L. G. Moss, G. N. Phillips Jr., *Nature Biotechnol.* **14**, 1246 (1996).
9. T. Ehrig, D. J. O'Kane, F. G. Prendergast, *FEBS Lett.* **367**, 163 (1995).
10. R. Heim, D. C. Prasher, R. Y. Tsien, *Proc. Natl. Acad. Sci. U.S.A* **91**, 12501 (1994).
11. R. Heim, A. B. Cubitt, R. Y. Tsien, *Nature* **373**, 663 (1995).
12. S. Delagrave, R. E. Hawtin, C. M. Silva, M. M. Yang, D. C. Youvan, *Biotechnology* **13**, 151 (1995).
13. The cDNA fragments coding for wild-type drFP583 and the E5 mutant were subcloned into pTRE2 vector (Clontech). The HEK 293 Tet-On or 293 Tet-Off cells (Clontech) were transiently transfected with a CalPhos kit (Clontech). Doxycycline at a final concentration of 2 g/ml was added after 24 or 48 hours for Tet-On or Tet-Off cells, respectively. Cells were analyzed by FACS Calibur (Becton Dickinson). The images were taken with a XF35 Omega filter set, using a cooled charge-coupled device camera and analyzed with MetaMorph Software (Universal Imaging).
14. D. Jones, D. K. Dizon, R. W. Graham, E. P. M. Candido, *DNA* **8**, 481 (1989).
15. An E5 cDNA was subcloned into pPD49.83 vector, which contains the *hsp16-41* promoter and a 3′ UTR derived from the *unc-54* gene. Germ line transformants were obtained by microinjection of a mixture of DNA containing the [*hsp-E5*(+)] transgene (100 μg/ml) and the *unc-29*(+) gene (F35D3, 100 μg/ml) into *unc-29*(*e1072*) mutant animals. Animals were heat-shocked by floating an agar plate containing the worms in a water bath preheated to 33°C. The images were taken with a Chroma Polycroich beamsplitter 86100bs filter set [for 4′,6′-diamidino-2-phenylindole, fluorescein isothiocyanate (FITC), and *R*-phycoerythrin (PE)] and analyzed with MetaMorph Software (Universal Imaging).
16. A. Terskikh *et al.*, data not shown.
17. P. G. Okkema, S. W. Harrison, V. Plunger, A. Aryana, A. Fire, *Genetics* **135**, 383 (1993).
18. B. Galliot, D. Miller, *Trends Genet.* **16**, 1 (2000).
19. G. V. Ermakova *et al.*, *Development* **126**, 4513 (1999).
20. Plasmids containing the E5 mutant under the control of the *Otx-2* and *Xanf-1* promoters were made as previously described (*2*). The fluorescence of the E5 mutant in *Xenopus* was visualized by FITC filter set B1 of the Polyvar photomicroscope (Reihert-Jung).
21. L. D. Etkin, B. Pearman, *Development* **99**, 15 (1987).
22. A. G. Zaraisky *et al.*, *Development* **121**, 3839 (1995).
23. We thank S. Cenk, G. Davis, L. Ding, and T. Duong for technical help; E. Boncinelli and A. V. Belyavsky for the *Otx-2* and *Xanf-1* promoters; and J. Remington, R. Tsein, and M. Davis for critical reading of the manuscript. Partially supported by grants from CRDF (no. RB1-2034) and FIRCA (no. 1 RO3 TW01362-01) to A.G.Z.

27 April 2000; accepted 17 October 2000

Oxygen Activation and Reduction in Respiration: Involvement of Redox-Active Tyrosine 244

Denis A. Proshlyakov,[1] Michelle A. Pressler,[1] Catherine DeMaso,[1] Joseph F. Leykam,[2] David L. DeWitt,[2] Gerald T. Babcock[1]*

Cytochrome oxidase activates and reduces O_2 to water to sustain respiration and uses the energy released to drive proton translocation and adenosine 5′-triphosphate synthesis. A key intermediate in this process, P, lies at the junction of the O_2-reducing and proton-pumping functions. We used radioactive iodide labeling followed by peptide mapping to gain insight into the structure of P. We show that the cross-linked histidine 240–tyrosine 244 (His^{240}-Tyr^{244}) species is redox active in P formation, which establishes its structure as Fe^{IV}=O/Cu_B^{2+}-H^{240}-Y^{244}•. Thus, energy transfer from O_2 to the protein moiety is used as a strategy to avoid toxic intermediates and to control energy utilization in subsequent proton-pumping events.

Respiration activates and reduces 95% of the O_2 that we consume. In this process, the terminal respiratory enzyme, cytochrome oxidase, couples exergonic dioxygen reduction to endergonic proton translocation to drive adenosine 5′-triphosphate synthesis. There is now a relatively good understanding of the cytochrome oxidase reaction cycle (*1*) in which O_2 binds and is eventually reduced to water (Fig. 1). However, the structure of a key intermediate, **P**, which lies at the intersection of the O_2 reduction phase and the proton translocation function, has not been determined. The major uncertainty pertains to the location of one of its strongly oxidizing equivalents, the reduction of which drives the initial events in proton pumping. Reduction of **P** involves at least two proton-controlled, one-electron reduction steps, **P**→**F** (ferryl oxo species) and **F**→**O** (ferric hydroxo species) (*2*), each of which conserves appreciable energy in the chemiosmotic gradient (*3*), although the details are controversial (*4*–*7*).

Spectroscopic analysis shows that **P** is a bond-cleaved Fe^{IV}=O species (*1*, *2*). Neither heme iron nor oxygen changes its oxidation state upon the **P**→**F** transition (*8*), however, which poses the question as to the location of the extra oxidizing equivalent in **P**. Formation of a long-lived (>10 μs) heme π-cation radical can be ruled out (*1*, *2*). Recent observations of a covalent cross-link between the Cu_B ligand, H^{240}, and Y^{244} in the vicinity of heme a_3 (Fig. 1) (*9*, *10*) suggested immediately the location of this oxidizing equivalent and provided a rationale for the lack of definitive electron paramagnetic resonance radical signatures in **P** as arising from exchange coupling between Y^{244} and Cu_B (*11*). However, the experimental observations can also be explained by formation of Cu_B^{III} or by magnetic interactions between Cu_B and heme a_3, if the radical is located elsewhere. The development of protein radicals in a small fraction of **P** species under some conditions has been reported (*12*–*17*), but the identity of these species and their catalytic relevance is unclear.

Because spectroscopic techniques ap-

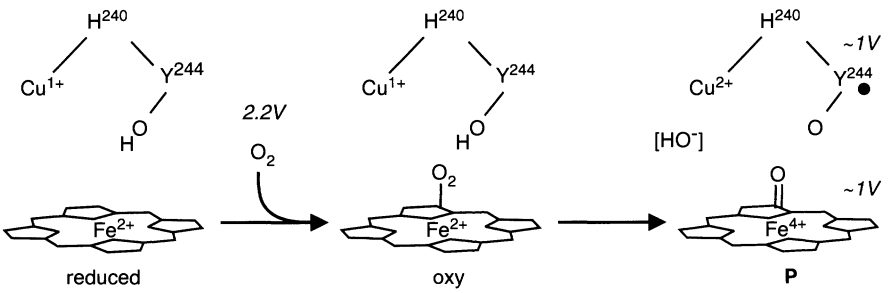

Fig. 1. Oxygen reduction and formation of **P** in the oxidative phase of the cytochrome oxidase/O_2 cycle. Only heme a_3 and the redox-active Cu_B-ligated Y^{244}-H^{240} cross-linked structure are shown. See (*11*, *33*, *34*) for details.

[1]Department of Chemistry and [2]Department of Biochemistry, Michigan State University, East Lansing, MI 48824, USA.

*To whom correspondence should be addressed. E-mail: babcock@cem.msu.edu